Acta Crystallographica Section D
Biological Crystallography
ISSN 0907-4449

Structures and comparison of the Y98H (2.0 Å) and Y98W (1.5 Å) mutants of flavodoxin (*Desulfovibrio vulgaris*)

Ross A. Reynolds,[a] William Watt[b]* and Keith D. Watenpaugh[b]

[a]Physics Department, Grand Valley State University, Allendale, Michigan, USA, and [b]Structural, Analytical and Medicinal Chemistry, Pharmacia Corporation, Kalamazoo, Michigan, USA

Correspondence e-mail: william.watt@pharmacia.com

Received 15 May 2000
Accepted 5 February 2001

PDB References: Y98H flavodoxin, 1i1o; Y98W flavodoxin, 1f4p.

The structures for two mutants at the Tyr98 site of *Desulfovibrio vulgaris* flavodoxin have been determined. The first, a tyrosine-to-histidine (Y98H) variant, was determined at the moderately high resolution of 2.0 Å, while the tyrosine-to-tryptophan variant (Y98W) yielded very high resolution data (beyond 1.5 Å) allowing a detailed look at the water structure, alternate side-chain conformations and the planarity of the FMN. Both structures were solved by molecular replacement beginning with the native (P2A) coordinates as a starting point. The Y98H variant of *D. vulgaris* flavodoxin crystallizes in space group $P2_12_12_1$, with unit-cell parameters a = 41.96, b = 61.45, c = 57.04 Å, while the Y98W mutant adopts space group $P2_1$, with a = 41.29, b = 55.82, c = 32.52 Å, β = 100.68°. Refinement for both mutants utilized *PROLSQ* followed by, for the high-resolution Y98W structure, anisotropic refinement as implemented in *SHELXL*. Final R factors of 17% for the Y98H mutant and 9.8% for the Y98W mutant were obtained. For the high-resolution (1.5 Å) Y98W mutant, 31 010 unique reflections were collected from a single crystal. The final model includes 273 solvent molecules, with eight side chains assuming multiple conformations. At this resolution, the detailed conformation of the FMN can be observed, with both a bow and twist being noted. A comparison is made between the two mutants and the different oxidation states of the native flavodoxin. Although both mutants show similar E_2 (oxidized/semiquinone) one-electron redox potentials to the native, the E_1 (semiquinone/hydroquinone) redox potential for the Y98H mutant is significantly different from that of the Y98W variant and the native protein. The surprising similarity in the folding of the polypeptide chain 60–64 between the two mutants and the reduced states of the native is discussed. The interaction between O61 and N5 in the flavin is discussed because of the new conformation of this loop.

1. Introduction

Flavodoxins are a class of low-potential electron-transfer proteins found in a variety of microorganisms. They substitute for iron–sulfur proteins such as ferredoxins in iron-deficient media (LeGall *et al.*, 1979). In other organisms, flavodoxins are produced constitutively. Flavodoxins fall into two classes according to their size. The physical properties, such as redox potential, of many of these proteins are well established and the tertiary structure of this protein is known from *Clostridium beijerinickii* (Ludwig *et al.*, 1997), *Desulfovibrio vulgaris* (Watenpaugh *et al.*, 1973), *Anacystis nidulans* (Smith *et al.*, 1983; Drennan *et al.*, 1999), *Chondrus crispus* (Fukuyama *et al.*, 1992), *Anabaena* 7120 (Burkhart *et al.*, 1995), *Escherichia*

coli (Hoover & Ludwig, 1997), *Desulfovibrio desulfuricans* (Romero *et al.*, 1996) and *Megasphaera elsdenii* (van Mierlo *et al.*, 1990). These proteins have similar polypeptide folding patterns, with a central β-sheet core flanked by pairs of α-helices. In an attempt to understand the mechanism of electron transfer, the reduced states of the *C. beijerinckii* (Smith *et al.*, 1977) and *D. vulgaris* (Watt *et al.*, 1991) flavodoxins have been examined by X-ray crystallography. From these studies, a flipping of the peptide chain is found to occur near N5 of the isoalloxazine ring in the reduced states. Since the gene for flavodoxin from *D. vulgaris* has been sequenced and cloned (Krey *et al.*, 1988), a comparison of the mutants of flavodoxin has been carried out and the residues believed to be responsible for regulating the redox potential of the semiquinone/hydroquinone redox couple have provided some interesting insights. As most flavodoxins have a tyrosine in the FMN-binding site, Tyr98 of the *D. vulgaris* flavodoxin was chosen to be modified (Swenson & Krey, 1994). Reported here are the structures and a comparison with the native structure of two of these mutations as determined by X-ray crystallography. These structures have also been studied using NMR (Stockman *et al.*, 1994). The Y98W mutant diffracted to higher resolution than any of the previously examined flavodoxins. With data better than 95% complete to 1.5 Å resolution, the quality of the resulting maps allows the study of the fine details of the structure with a high degree of confidence. Precise main-chain and side-chain positions, residues occupying multiple conformations, detailed solvent structure and precise information on the extent of bow of the FMN are presented. The high-resolution data allows the details of the conformational changes believed to be caused by the mutation to be easily observed.

2. Methods

2.1. Crystallization and data collection

Crystals of Y98H flavodoxin were grown from 3.1 *M* $(NH_4)_2SO_4$ buffered with 0.1 *M* Tris–HCl pH 7.5. The Y98W crystals were grown from 3.2 *M* $(NH_4)_2SO_4$ buffered with 0.1 *M* Tris–HCl pH 7.0. Crystals acceptable for diffraction studies were obtained using protein concentrations between 0.8 and 1.0%. Both mutant crystals required a few weeks to a few months to grow to a suitable size for diffraction measurements. The Y98H crystals were generally single, while the Y98W crystals appeared as clusters of rectangular cross-section rods growing from a common nucleation site. In all cases, the Y98W crystals had to be cut for diffraction studies. For each structure, the data were collected from a single crystal. Data for the structure determinations were collected using a Siemens P4/Xentronics area detector with Cu $K\alpha$ radiation produced by a Siemens rotating-anode generator and a vertical graphite monochromator. Statistics of data collection are presented in Table 1. All data were collected at room temperature (296 K) and processed with version 2.0 of the *XENGEN* software package (Howard *et al.*, 1987). Crystals for both mutants were very stable in the X-ray beam, with no noticeable degradation in the quality of the data during overnight data collection on the area detector. For the high-resolution Y98W mutant, the 1.5 Å resolution assigned to the structure reflects the $I/\sigma(I) = 1.0$ limit of 1.47 Å. Good quality data with $I/\sigma(I)$ values above 2.0 extending to a resolution cutoff of 1.3 Å were used in the *XTAL* and *PROLSQ* refinement, while all data except specifically identified outliers were used for the anisotropic *SHELXL* (Sheldrick & Schneider, 1997) refinement, as advocated by Sheldrick in the *SHELXL* manual. The $R_{\rm merge}$ for all reflections was 0.058 (unweighted absolute *R* factor on *I*), with the data being better than 95% complete to 1.5 Å resolution.

2.2. Structure solution and refinement

The Y98H and Y98W mutant structures were solved using molecular replacement. The oxidized room-temperature structure of native (P2A) *D. vulgaris* flavodoxin (Watt *et al.*, 1991) was used as a probe molecule. The *MERLOT* system of programs (Fitzgerald, 1988) was used to complete the rotation (Lattman & Love, 1972; Crowther, 1972) and translation (Crowther & Blow, 1967) search as well as to apply the resulting values. Translational solutions were found based on 8σ rotation solutions for the Y98H and a single 11σ solution for the Y98W mutant. Refinement for the Y98H mutant utilized *PROLSQ* (Konnert & Hendrickson, 1980; Sheriff, 1987) on data with $I > 2\sigma(I)$ in a final resolution range of 8–2.0 Å, while refinement of the Y98W mutant utilized *CEDAR* (Watenpaugh, 1985) as incorporated in the *XTAL* system of programs (Hall *et al.*, 1992) and *PROLSQ* for data with $I > 2\sigma(I)$, both in a final resolution range of 20–1.3 Å. Anisotropic refinement with *SHELXL* included all data in the resolution range 8.0–1.3 Å. Model rebuilding was performed initially on an Evans & Sutherland PS390 computer graphics system running *FRODO* software (Jones, 1985; Pflugrath *et al.*, 1985) using $2F_o - F_c$ and $F_o - F_c$ electron-density maps and later on an Silicon Graphics Indigo using the programs *CHAIN* (Sack & Quiocho, 1997) and *LORE* (Finzel, 1997). All electron-density maps used Sim (1960) weighting in order to reduce aberrant calculated phases from Fourier syntheses.

Refinement of the Y98H mutant was complete after 94 cycles and five rebuilding sessions with data in the resolution range 8–2.0 Å and an *R* factor ($I > 2\sigma$) of 17.4%. The Y98H model incorporates 141 sites for solvent atoms. Solvent atoms were only added when reasonable density appeared in both $2F_o - F_c$ and difference maps and if at least one hydrogen bond to a donor was present. Occupancies and thermal parameters of the solvent were refined in alternating cycles. A summary of the refinement statistics is shown in Table 1. The atomic coordinates and structure-factor data have been deposited in the Protein Data Bank (Berman *et al.*, 2000). Refinement of the Y98W mutant began using *CEDAR* starting from an 8σ translation-search peak. The initial F_c calculation using this model had an *R* factor of 37% and incorporated data to 2.5 Å. *CEDAR* can refine molecular structures using energy minimization and crystallographic techniques either separately or in conjunction with each other.

We have found that it allows rapid inclusion of high-resolution data and in our environment has worked well for looking at small changes in structures such as the binding of different inhibitors to a particular protein. Refinement with *PROLSQ* was begun because of difficulty in modeling some alternate side-chain conformations, particularly Arg131, where the two conformations of the side chain slowly diverge starting from the C^{β}, and because of the need to compare final structural statistics with those of the native and Y98H mutant which had been refined with *PROLSQ*. Finally, *SHELXL* was used because of its ease of specification of alternate configurations and ability to refine anisotropically. In all cases, refinement sessions were interspersed with model-building sessions using *FRODO* or *CHAIN* with the incorporation of *LORE*. The final *SHELXL* model incorporates eight alternate conformation side chains and 273 solvent molecules. Final R factors [$I > 2\sigma(I)$] from *CEDAR*, *PROLSQ* and *SHELXL* are 16.2, 16.6 and 9.8%, respectively. Crystallographic parameters and final refinement statistics for all are presented in Table 1.[1] Coordinates from the *SHELXL* model were deposited in the Protein Data Bank.

Refinement with *SHELXL* was started in part to develop experience with this program and in part to assess the ease with which one could specify and refine alternate conformations. Following initial isotropic (conjugate-gradient least-squares) refinement, the R factor [$I > 2\sigma(I)$] stabilized at 15.4% with an $R_{\rm free}$ of 20%. This model included eight alternate side chains modeled using the PART I and PART II instructions with different names for the atoms in the alternate chains and SADI to ensure proper geometry. The 1997 *SHELXL* release removes the need for different atom names, making alternate side-chain specification easier. This isotropic structure included 233 solvent molecules. All refinements were run without bulk-solvent correction. The *SHELXL* refinement used antibumping restraints of 2.0 Å for solvent atoms. At this point, following the procedure outlined in Sheldrick's *SHELXL* manual, the data were tested to determine whether anisotropic refinement was justified. The $R_{\rm free}$ fell by 2%, a fall of 1% being the suggested decision criterion for proceeding with anisotropic refinement. With 147 residues and the FMN, we carried out the anisotropic refinement in block mode, specifying blocks of about 15 residues overlapping by four or five residues with adjacent blocks. Completion of the first successful run brought the R factor to 12.7%. The data-to-parameter ratio for this anisotropic refinement was 24 812:12 790 or about 2:1. Further cycles of modeling and refinement brought the R factor to 11.2%. At this point, calculated H atoms were added which further reduced the R factor. Model building and further refinement, including addition of more solvent aided by the solvent-suggestion routines built into *SHELXL*, resulted in an R factor below 10%. To remove any possible artifacts caused by block refinement, a final run of four cycles of conjugate-gradient least-squares refinement on the whole structure was performed. The final model has R factors of 9.8% [$I > 2\sigma(I)$] and 12.7% (all data) and an $R_{\rm free}$ of 16.8% (all data). Inclusion of data to 1.3 Å, even though the average $I/\sigma(I)$ for this shell is less than unity, was driven by the large number of observed reflections and reflections above 2σ for the 1.5–1.3 Å shell. Of the theoretical 18 242 reflections, 13 450 were observed and 26% of these, or 3531, had intensities of 2σ or greater. The 2σ

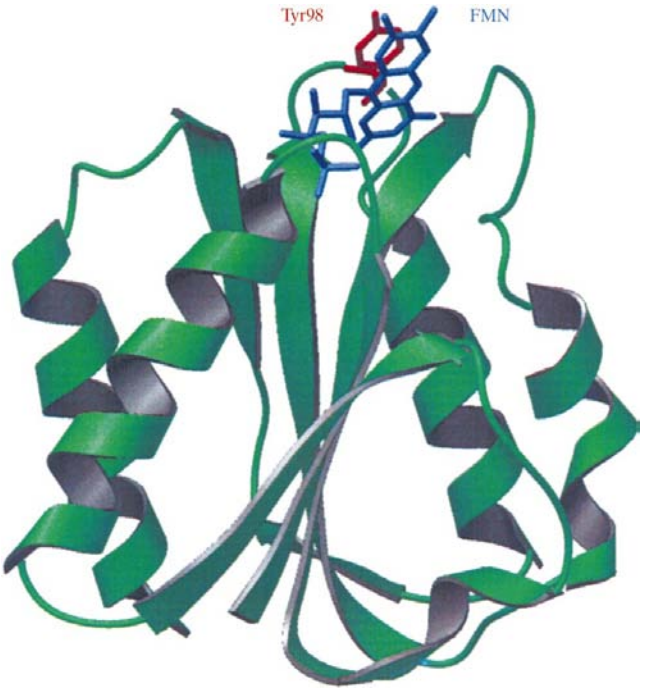

Figure 1
Ribbon drawing of flavodoxin (P2A) indicating the site of the mutations for Y98W and Y98H (red). The flavin is shown with standard atom colors in tube format.

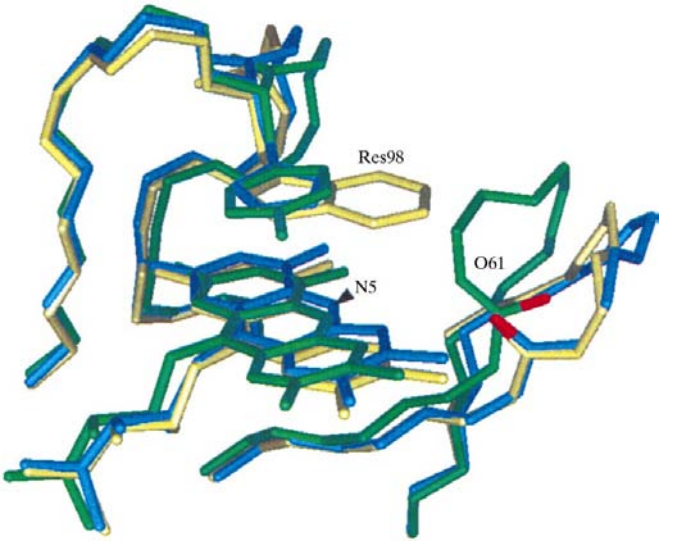

Figure 2
Flavin, mutation site and position of the 60–64 loop for the native oxidized (green), Y98H (blue) and Y98W (yellow) forms of the flavodoxin protein. O61 is shown in red.

[1] Supplementary material has been deposited in the IUCr electronic archive (Reference: sx0039). Details for accessing these data are described at the back of the journal.

cutoff limit is only used in *CEDAR* and *PROLSQ*, with *SHELXL* using all observed data for refinement (except, of course, the reflections which were omitted for calculation of R_{free}). The 9.8% R factor for data with $I > 2\sigma$ produced by *SHELXL* is calculated for comparison with other refinements where this restriction is placed on data. The final *SHELXL* model incorporates eight residues modeled with alternate confirmations and a total of 273 solvent molecules. Although we were able to drive both R_{free} and R somewhat lower with additional solvent modeling, we limited solvent molecules to those that passed the criterion that $B_{isotropic}$/occupancy < 100. The omission of every 75th reflection for calculation of R_{free} was started at the beginning and continued for the entire course of the *SHELXL* refinement. As this structure was already well refined through *CEDAR* and again with *PROLSQ*, we included all data from the outset of *SHELXL* refinement, thus preserving the integrity of the reflections held back to calculate R_{free} throughout the *SHELXL* refinement. The fact that many of these reflections were used in the earlier refinements may have resulted in slightly different R_{free} values than if these reflections had been held out from the beginning of all refinements.

Table 1
Crystallographic and refinement parameters.

A summary of selected *CEDAR*, *PROLSQ* and *SHELXL* refinement and *PROCHECK* statistics. Mean values of bond lengths and angles are given followed by r.m.s. deviations in parentheses.

Compound	P2A(native)	Y98W			Y98H
Space group	$P4_32_12$	$P2_1$			$P2_12_12_1$
Unit-cell parameters					
a (Å)	51.96	41.29			41.96
b (Å)	51.96	55.82			61.45
c (Å)	139.86	32.52			57.04
β (°)	90.00	100.68			90.00
No. of reflections [$I > 2\sigma(I)$]	11964	18955			9294
Resolution (Å)	20.0–1.9	20.0–1.30			8.0–2.0
Completeness (resol.)		95% (1.5 Å)	85% (1.3 Å)		
$I/\sigma(I)$ (shell, Å)		1.0 (1.49–1.47)	0.73 (1.29–1.30)		
Refinement program	*PROLSQ*	*PROLSQ*	*CEDAR*	*SHELXL*	*PROLSQ*
R factor	0.170	0.166	0.162	0.098	0.172
R_{free}				0.168	
Model deviations					
Bond (Å)	0.024	0.015	0.019	0.018	0.013
Angle (Å, °)	0.054	0.031	2.8	2.12	0.025
Planar 1-4 (Å, °)	0.050	0.045	5.4		0.022
Solvent molecules	130	187	168	273	140
Alternate conformations		3	7	8	
Main-chain bond lengths (Å)					
C—N		1.33 (0.01)	1.32 (0.01)	1.33 (0.02)	1.32 (0.01)
N—C^{α}		1.48 (0.02)	1.47 (0.02)	1.46 (0.02)	1.47 (0.01)
C—O		1.24 (0.02)	1.24 (0.01)	1.22 (0.02)	1.24 (0.01)
C^{α}—C (except Gly)		1.53 (0.02)	1.54 (0.02)	1.52 (0.02)	1.53 (0.01)
C^{α}—C^{β}		1.53 (0.02)	1.53 (0.02)	1.53 (0.02)	1.53 (0.02)
Main-chain bond angles (°)					
C—N—C^{α} (except Gly, Pro)		120.7 (2.6)	121.6 (2.2)	120.0 (1.9)	123.2 (2.6)
C^{α}—C—N (except Gly, Pro)		115.6 (2.9)	115.7 (2.4)	115.5 (2.1)	115.7 (2.0)
C^{α}—C—O (except Gly)		119.5 (2.5)	120.5 (2.4)	121.0 (1.8)	120.0 (1.9)
N—C^{α}—C^{β} (except Gly, Pro)		109.8 (3.1)	110.0 (3.5)	110.0 (2.2)	111.5 (3.0)
O—C—N (except Pro)		124.7 (2.9)	123.6 (2.0)	123.4 (2.1)	124.1 (1.5)
Dihedral angles (°)		180.0 (3.3)	179.6 (6.2)	180.3 (4.3)	179.7 (2.7)
Ramachandran plot					
% Most favored		92.8	94.0	96.7	94.4
% Allowed (disallowed)		6.2 (0.0)	6.0 (0.0)	3.3 (0.0)	5.6 (0.0)

3. Results and discussion

3.1. Overall structure

The overall shape of the molecule is displayed as a ribbon diagram of the backbone of the native (P2A in green) in Fig. 1. The site of the mutation (Tyr98) is shown in red. Parallel β-strands comprise the core of the protein and the two pairs of α-helices lie on each side of the β-strands to form a classic α/β structure. As Tyr98 resides near the surface of the protein, one would not expect mutagenesis at this position to result in a large conformational change of the entire molecule. Indeed, the bulk of the folding did remain the same in each mutant when compared with the native.

The major change noted during initial stages of refinement was a shift in position of the 60–64 loop away from the site of mutation. This shift results from rotation of the polypeptide chain 61–62 such that O61 points toward N5 of the isoalloxazine ring as in the conformation discovered in the reduced states of the native. Fig. 2 shows this loop in the native (green), Y98H (blue) and Y98W (yellow) and the region around the mutation. For the Y98W variant, the r.m.s. deviation of this loop from the native is 1.6 Å, with the largest main-chain movement occurring in Asp62, which has an r.m.s. main-chain difference of 3.8 Å and side-chain difference of 5.8 Å from the native structure. Crystal packing was investigated because of the space-group differences from the native structure, but for both mutants no atoms or ordered water associated with neighboring molecules appeared to be in a position to cause the shift of the 60–64 loop. The shift is stabilized in the Y98W variant structure by a hydrogen bond between Asp62 $O^{\delta1}$ and Lys113 N^{ζ} in a neighboring molecule, but because of the large side-chain shift required to establish this bond we feel this hydrogen bond is unlikely to be the cause of the shift, but rather a consequence of it. Therefore, the structural shift of this loop is likely to be a result of the mutation from the native to the Y98W variant. No such intermolecular interaction is seen in the Y98H variant or the native structure.

Crystal packing may be the cause for the positional change of the 97–102 loop, whose main-chain r.m.s. is greater than

Table 2
Hydrogen bonds and close contacts between the FMN and the apoprotein or solvent of Y98H (Y98W).

FMN	Apoprotein/solvent	Distance (Å)
N1	N 95	3.27 (3.27)
N3	O 100	2.62 (2.81)
N5	O 61	4.19 (4.08)
O2	N 95	3.08 (3.07)
O2	N 102	2.79 (2.78)
O4	Wat 172 (203)	3.10 (2.77)
O2′	O 59	2.81 (2.59)
O4′	$N^{\gamma 2}$ 14	2.95 (2.83)
O4′	Wat 189 (205)	2.86 (2.75)
O6′	O_{γ} 10	2.91 (2.64)
O6′	N 15	2.84 (2.63)
O7′	$O^{\gamma 1}$ 12	2.89 (2.59)
O7′	N 14	2.75 (2.95)
O8′	N 11	2.69 (2.71)
O8′	O^{γ} 58	2.74 (2.59)

1 Å. In this loop of the Y98W variant, Tyr100 has an r.m.s. difference of 1.6 Å in position from the native structure and this loop, containing the mutation, is in close contact (<3.5 Å) with a neighboring molecule. Tyr100 OH forms a hydrogen bond with Gln84 $N^{\varepsilon 2}$ in the neighboring molecule in this mutant structure. No other non-terminal residues had observed r.m.s. deviations from the native of greater than 1 Å.

Final refinement showed that the hydrogen-bonding scheme (Table 2) of the ribityl and phosphate groups of the FMN showed little change between the native and mutants; however, the hydrogen-bonding network around the FMN is somewhat different. Both mutant structures showed slight bending in the isoalloxazine ring of the FMN. The angle between the plane normals of the two outer rings is 7.5° (Y98H) and 7.4° (Y98W), respectively.

3.2. Quality of mutant structures

The overall quality of the Y98W and Y98H structures was assessed with the *PROCHECK* program (Laskowski *et al.*, 1993). Table 1 summarizes the assessment of the Y98H mutant structure as well as final *CEDAR*, *PROLSQ* and *SHELXL* determined models for the Y98W mutant. Also presented in this table are the corresponding parameters for the native (P2A) form of the protein. In using *PROCHECK* for the Y98W structures, multiple conformations were not considered and the models were modified to have only single side-chain conformations placed in the conformation of highest occupancy. It is clear from the similarity of the end models and the *PROCHECK* assessment that all three programs arrived at fully satisfactory models for the Y98W mutant of the protein.

Comparison of temperature factors between the different mutant models shows the expected correlation of low relative temperature factor for the β-sheet core of the protein as well as the expected higher temperature factors for the α-helices and β-turns which mostly comprise the surface of the protein. The average temperature (B) factors for the protein atoms, FMN atoms and water molecules from the *PROLSQ* model of the Y98H mutant are 13.5, 8.0 and 18.7 $Å^2$, respectively, while those for Y98W obtained from *PROLSQ* were 14.4, 8.9, and 18.8 $Å^2$, respectively, and those based on calculated isotropic Bs generated for the anisotropic model of the Y98W mutant by *SHELXL* are 20.0, 13.0 and 39.5 $Å^2$, respectively. The general difference in these values is felt to be one caused by program differences in approach to temperature-factor refinement and scaling. The large discrepancy for the solvent molecules reflects the additional weaker solvent assignments made in the anisotropic phase of refinement and the strategy in *SHELXL* of creating a web of fully occupied solvent molecules with higher temperature factors. For the purposes of further discussion and structural comparison with the native protein, the *SHELXL* model of Y98W has been used.

Table 3
Results of superpositions of different structures.

Numbers are in ångströms$_{\rm r.m.s.}$ for total/main-chain/side-chain residues

	Native	SQ	Y98H	Y98W (*SHELX*)
Native	0/0/0	0.60/0.33/0.80	1.0/0.47/1.4	0.85/0.47/1.1
SQ		0/0/0	1.1/0.61/1.5	0.97/0.59/1.3
Y98H			0/0/0	0.76/0.31/1.1
Y98W (*SHELX*)				0/0/0

3.3. Comparison of mutant and native structures

A superposition of Y98W on Y98H based on alignment generated by *SUPERIMP* (Honzatko, 1986) indicated an average r.m.s. difference for the main-chain atoms of 0.31 Å, while that of the side chains is 1.05 Å. The main regions of differences in the two structures are shown in Fig. 2. Table 3 summarizes the results of similar superpositions of the Y98H mutant with the oxidized and semiquinone forms of the native and of the Y98W mutant on both forms of the native. As demonstrated by the results from *SUPERIMP*, overall the mutant structures are more similar to each other than to the native forms of the protein. Comparison of the Ramachandran angles for the peptide chain 60–64 of the two mutants to those of the native structures (Table 4) indicates a greater similarity of the mutants, in this loop region, to the semi-reduced state than to the oxidized form of the native. In all three cases (Y98H, Y98W and semi-reduced native), the 60–64 loop is configured so that O61 points generally toward N5 of the FMN. This configuration, referred to as the 'O-up' configuration, is seen in many semi-reduced forms of a variety of both long- and short-chain flavodoxins (Smith *et al.*, 1977; Watt *et al.*, 1991; Ludwig *et al.*, 1997; Hoover *et al.*, 1999).

Figs. 3(*a*), 3(*b*), 3(*c*) and 3(*d*) show stereoviews of this loop region including residues 61, 62, surrounding solvent and N5 of the FMN for the native oxidized, native semi-reduced, Y98H and Y98W forms of the protein. Although Wat155 appeared in all three oxidation states of the native, bridging O4 of the FMN to O62 and N100 (Watt *et al.*, 1991), this scheme has changed for the two mutants. In Y98H, two waters, Wat231 and Wat172, appear in the vicinity of Wat155 of the native; their presence might arise from reordering owing to the greater solvent-accessible volume. In Y98W, Wat203, Wat220 and Wat208 appear in this same region, indicating a completely different hydrogen-bonding scheme.

In the case of the reduced forms of the native protein, O61 forms a hydrogen bond with N5 of the isoalloxazine ring. The Y98H and Y98W mutants have the same O61 ('O-up') in the same orientation as to hydrogen bond with N5, except the polypeptide chain has moved away so that a direct hydrogen bond could not be formed. The distances between O61 and N5 are 4.19 and 4.08 Å for the Y98H and Y98W mutants, respectively. An indirect or bridging hydrogen bond through Wat203 in the Y98W or the equivalent solvent molecule in the Y98H structure is non-ideal because of the observed geometry and distances (O61—Wat203—N5 angle less than 90°, Wat203—N5 distance is 3.22 Å in Y98W). Considering the large number of hydrogen-acceptor groups (four within 3.0 Å) and the electrostatically negative environment, it appears likely that Wat203 might be an ammonium ion rather than a water molecule. In the refined structure, this site is represented by a fully occupied O atom and has a quite reasonable temperature factor of 11 Å^2 (Fig. 3*d*).

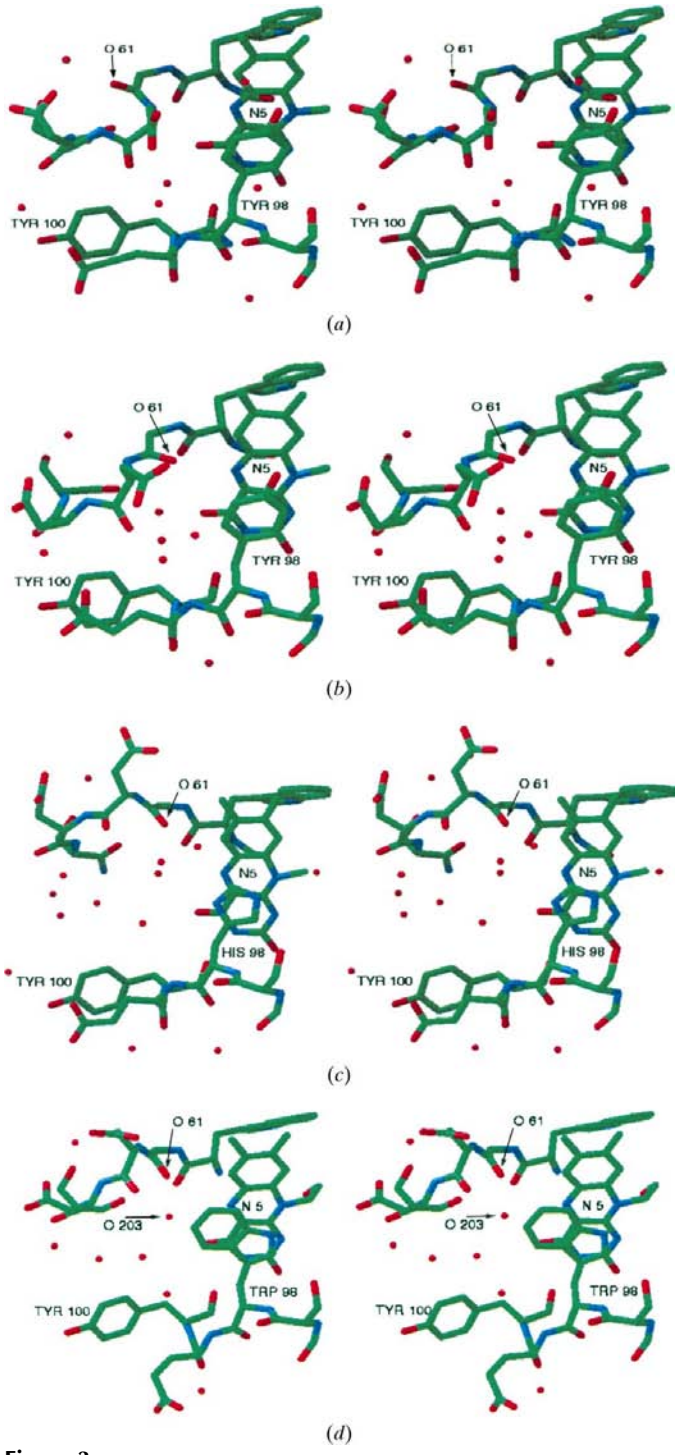

Figure 3
Stereoviews of the region surrounding N5 of the flavin and loops 60–64 and 97–100 with solvent atoms. (*a*) Native (P2A) oxidized form of the protein, (*b*) semi-reduced form of the P2A protein, (*c*) Y98H mutant, (*d*) Y98W mutant.

Table 4
Selected Ramachandran angles for Y98H, Y98W and native.

Angles (°)	Y98H	FlavodoxinY98W	Native (P2A)	
			Oxidized	Semiquinone
φ_{60}	131	134	127	130
ψ_{60}	158	166	176	176
φ_{61}	103	109	104	102
ψ_{61}	139	139	−42	163
φ_{62}	−84	−61	70	115
ψ_{62}	−49	−57	−69	−64
φ_{63}	130	154	−83	105
ψ_{63}	10	47	−16	1
φ_{64}	159	154	143	125
ψ_{64}	165	47	179	154

The 60s loop is two residues longer than the corresponding loops in other flavodoxins; this difference might allow greater flexibility for interacting with other electron-transport proteins. Mutation of residue 61 to alanine (G61A; O'Farrell *et al.*, 1998) results in a large shift in the ox/sq potential (E_2) and a large movement of this loop, which may be necessary to remove bad contacts introduced by the mutation. This large loop movement is not observed if the glycine residue equivalent to Gly61 is mutated to Ala, Asp or Asn in the shorter-looped flavodoxin *C. beijerinckii* (O'Farrell *et al.*, 1998; Ludwig *et al.*, 1997). A comparison of these three structures (Y98W, G61A and *C. beijerinckii*) is shown in Fig. 4.

Because of the several conformations of the 60s loop in the *D. vulgaris* mutants (Tyr98, Gly61), it appears that there are only small energy differences between them as suggested for the corresponding loop region in flavodoxin from *C. beijerinckii* (Ludwig *et al.*, 1997). A correlation between the hydrogen bond to N5 and the redox potential for E_2 has been discussed based on a small data set (Fukuyama *et al.*, 1992). That is, in the native *D. vulgaris* and *C. beijerinckii* proteins (E_2 of −102 and −92 mV, respectively), a new hydrogen bond is formed upon reduction to the semiquinone state. However, in *Chondrus crispus* and *Anabaena* 7120 (E_2 of −235 and −196 mV, respectively) a hydrogen bond exists in the oxidized state. The E_2 for the *D. vulgaris* flavodoxin of −102mV is higher than the −146mV value subsequently reported (Curley *et al.*, 1991). The Y98H and Y98W mutants of the *D. vulgaris*

protein have E_2 values of −175 and −152 mV, respectively (Table 5) (Swenson *et al.*, 1991). Both Y98W and Y98H mutants show the peptide chain already oriented for a hydrogen-bond interaction with N5 (albeit an indirect one) in the oxidized state. It appears that this chain reorientation and hydrogen-bond formation might be in place so that the formation of the semiquinone is stabilized to allow the value of E_2 in the *D. vulgaris* system to increase. However, the hydrogen-bond distance is too long in the oxidized state for these two mutants and the crucial experiment to determine the effects of this hydrogen bond would be to study the reduced structures of these mutants and determine whether there is an adjustment bringing O61 closer to N5.

A comparison of the NMR order parameters with *B* factors from the X-ray structure of the oxidized and reduced protein shows higher values for the reduced form compared with the oxidized form, especially throughout the 55–63 and 92–103 loop regions (Hrovat *et al.*, 1997). When examining this same region of the Y98W and Y98H mutants, there is an increase in *B* factors in the 60–66 and 96–100 regions, with averages of 20 and 18 Å^2 for Y98H, and 19 and 17 Å^2 for Y98W, respectively. This can be compared with the average *B* factor for the protein of 13.5 Å^2 for Y98H and 14.4 Å^2 for Y98W. Although the *B* values for these loop regions are higher, there are no intermolecular contacts that influence this region.

The chain following Trp98 also exhibits some displacement, which at first glance appears to be sterically driven to accommodate the larger Trp side chain (Fig. 3). However, this displacement also occurs in the Y98H mutant, with its smaller side chain. The latter would seem to imply that additional structural studies of other mutant structures at Tyr98 might reveal the nature of what is driving this movement.

The environment of the isoalloxazine ring is somewhat different in each of the mutants of *D. vulgaris*. Since Tyr98 is coplanar with the outer portion of the flavin ring, there is a possibility that charge-transfer transition could occur between the π-clouds of the two ring systems. When this residue is substituted with tryptophan and histidine using standard point-mutagenesis methods, a slight change in redox potential for E_2 in the first case and a significant change for the second case are observed (Table 5) (Swenson *et al.*, 1991). Although the conformations of the Y98W and Y98H mutants appear similar, the His mutant exhibits significant redox-potential differences in E_2 when compared with the native. This could be a result of electrostatic effects with the flavin semiquinone since the two aromatic ring systems are different. The Y98W and Y98H mutants, when compared with the wild type, show a slight change in the E_1 in the first case and a large change in the second case (Table 5). Swenson & Krey (1994) have observed a linear dependence of the ox/sq couple (E_2) on pH over the range 5.5 to almost 9.0 (*ca* ∼60 mV per pH-unit increase) for the Y98H variant. They conclude that if titration of the imidazole ring occurs over this pH range, then there would appear to be no preferred interactions between either the neutral or the protonated forms of the histidine with the neutral flavin semiquinone in this variant. For the sq/hq couple, an approximate 180 mV electropotential increase relative to the wild type is observed at pH 7, but above pH 6 the potential begins to decrease with increasing pH. From these studies, Swenson & Krey suggest that stabilization of the hydroquinone anion by the positively charged histidine, less shielding of the flavin from solvent and favorable electrostatic interactions might account for the large difference in E_1 for the Y98H variant.

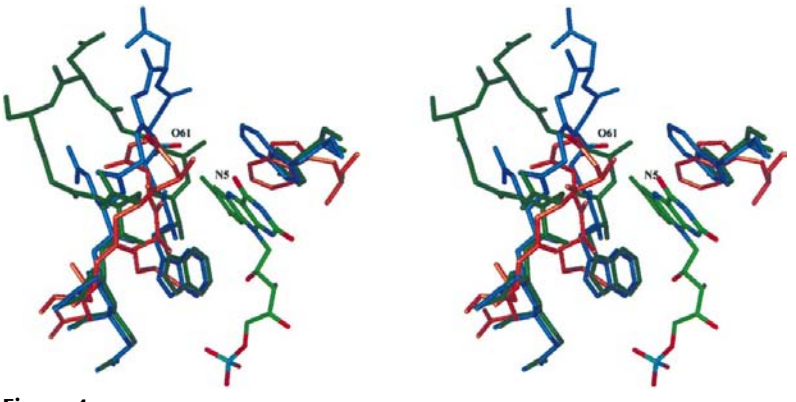

Figure 4
Stereo overlay of the FMN region for Y98W (*D. vulgaris*) (blue), G61A (*D. vulgaris*) (green) and *C. beijerinckii* (gold).

3.4. Details of the high-resolution Y98W mutant structure

3.4.1. Alternate conformations. As a result of the high-resolution data for the Y98W mutant, several residues occupying multiple conformations have been identified. For the purpose of r.m.s. comparison with the native, the mutant conformation with the highest occupancy was chosen. The residues that required multiple conformations were Arg24, Glu25, Ser35, Ser40, Val88, Ser97, Ile126 and Arg131. With the exception of Val88 and Ile126, these residues all lie on the surface of the protein. A representative view of Val88 with electron density is shown in Fig. 5. Occupancies for all residues exhibiting multiple conformation were refined and alternate conformations were generally not equally populated.

3.4.2. The flavin. The quality of the electron-density map for the Y98W mutant is displayed in Fig. 6, which gives two views of the FMN group. The $2F_o - F_c$ map is contoured at a level of 1σ and clearly indicates the position of all non-H atoms for the FMN. The second view clearly shows that the FMN rings are bowed as has been suggested previously (Smith *et al.*, 1977; Massey & Hemmerich, 1980; Watt *et al.*, 1991). Although both mutant structures appear to have a bow in the FMN ring structure, as did the native structure, it is only with high-resolution data that one feels comfortable in calculating a reliable bow angle for the rings. At this resolution, the amount of bow can be calculated as 7.4°. From a survey of 55 flavins (Lennon & Ludwig, 1999), the average of 7.0 ± 5.2° for oxidized flavins and 8.2 ± 5.9° for reduced flavins is in good agreement with what we have observed. This figure, determined using the *LSQPL* (Davenport & Flack, 1992) module of the

Table 5
Oxidation–reduction potentials for *D. vulgaris* flavodoxin mutants.

Values are in mV *versus* NHE, pH 7.0

Flavodoxin	E_2 (Ox→Sq)	E_1 (Sq→Hq)
Native	−146† (−102‡)	−443
Y98F	−148	−414
Y98W	−152	−449
Y98H	−175	−268
Y98R	−173	−272
Y98M	−206	−302
Y98A	−178	−304

† Curley *et al.* (1991). ‡ Fukuyama *et al.* (1992).

XTAL system, was generated by calculating the angle between least-squares planes determined from the atoms in the end rings of the FMN and represents the overall FMN bow, not a deviation of individual atoms of the FMN from planarity. The angle may be underestimated because planarity restraints in the refinement result in a slightly more planar geometry of the FMN than the $2F_o - F_c$ electron density appears to indicate. As this angle is calculated for a mutant structure, it may not reflect the degree of bow of the native but may rather be a product of the changes caused by the mutation or crystal packing. The latter seems somewhat less likely owing to the buried nature of the FMN.

4. Conclusions

The refinement of the Y98H and Y98W mutants of flavodoxin provides some insights into the redox potentials of the system. The redox potentials for the Y98W mutant are very similar to those of the native, while the structure in the region of the FMN, particularly near N5, has changed considerably. It would appear that the redox potential E_2 is relatively unperturbed by changes in the conformation of the oxidized flavodoxin that result from the mutations Y98H and Y98W. The high resolution of the Y98W structure coupled with the ability to complete anisotropic refinement using *SHELXL* allows the generation of maps of sufficient quality to look at solvent structure, assign multiple conformations to side chains and to study with some confidence the planarity and interactions of the FMN. The movements in response to the mutations appear to require the protein to crystallize in different lower symmetry space groups. Finally, as stated earlier, study of the reduced structures of these mutants would be useful for determining whether there is a conformational change bringing O61 closer to N5 and how the large differences observed in E_1 for the Y98H mutant are related to structure.

Figure 5
Representative view of electron density around Val88 with essentially equally occupied alternate conformations. Density is $2F_o - F_c$ contoured at 1σ.

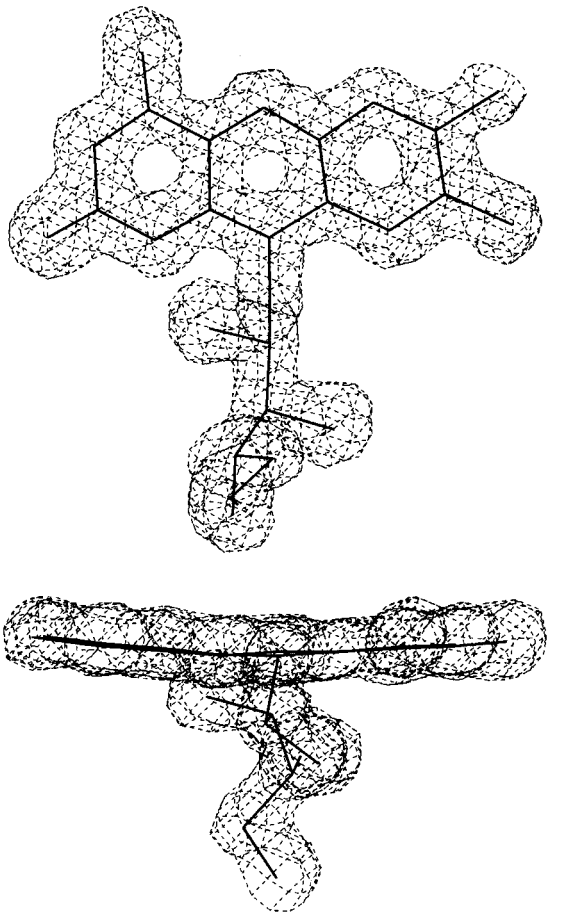

Figure 6
Two views of the flavin rings with $2F_o - F_c$ density for the Y98W mutant. Quality of electron-density maps is clearly shown as is the bow in the flavin.

We thank Dr Barry C. Finzel from of Phamacia Corporation for providing useful software and advice and Dr Richard P. Swenson of Ohio State University for providing us with the Y98W and Y98H forms of the protein. Support for R. Reynolds was provided in the form of travel reimbursement by a grant from Grand Valley State University Research and Development Committee. Resources at Grand Valley State University were provided through NASA under the Joint Venture (JOVE) program. Primary resources necessary to

complete this project were made accessible by the Pharmacia Corporation.

References

Berman, H. M., Westbrook, J. K., Feng, Z., Gilliland, G., Bhat, T. N., Weissig, H., Shindyalov, I. N. & Bourne, P. E. (2000). *Nucleic Acids Res.* **28**, 235–242.

Burkhart, B. M., Ramakrishnan, B., Hongao, Y., Reedstron, R. J., Markley, J. L., Straus, N. A & Sundralingram, M. (1995). *Acta Cryst.* D**51**, 318–330.

Crowther, R. A. (1972). *The Molecular Replacement Method*, edited by M. G. Rossmann. New York: Gordon & Breach.

Crowther, R. A. & Blow, D. M. (1967). *Acta Cryst.* **23**, 544–548.

Curley, G. P., Carr, M. C., Mayhew, S. G. & Voordouw, G. (1991). *Eur. J. Biochem.* **202**, 1091–1100.

Davenport, F. & Flack, H. D. (1992). *Xtal*3.2 *Reference Manual*, edited by S. R. Hall, H. D. Flack & J. M. Stewart. Universities of Western Australia, Geneva and Maryland.

Drennan, C. L., Pattridge, K. A., Weber, C. H., Metzger, A. L., Hoover, D. M. & Ludwig, M. L. (1999). *J. Mol. Biol.* **294**, 711–724.

Finzel, B. C. (1997). *Methods Enzymol.* **277**, 230–242.

Fitzgerald, P. M. D. (1988). *J. Appl. Cryst.* **21**, 273–278.

Fukuyama, K., Matsubara, H. & Rogers, L. J. (1992). *J. Mol. Biol.* **225**, 775–789.

Hall, S. R., Flack, H. D. & Stewart, J. M. (1992). Editors. *Xtal*3.2 *Reference Manual*. Universities of Western Australia, Geneva and Maryland.

Honzatko, R. B. (1986). *Acta Cryst.* A**42**, 172–178.

Hoover, D. M., Drennan, C. L., Metzger, A. L., Osborne, C., Weber, C. H., Pattridge, K. A. & Ludwig, M. L. (1999). *J. Mol. Biol.* **294**, 725–743.

Hoover, D. M. & Ludwig, M. L. (1997). *Protein Sci.* **12**, 2525–2537.

Howard, A. J., Gilliland, G. L., Finzel, B. C. & Poulos, T. L. (1987). *J. Appl. Cryst.* **20**, 383–387.

Hrovat, A., Blümel, M., Löhr, F., Mayhew, S. G. & Rüterjans, H. (1997). *J. Biomol. NMR*, **10**, 53–62.

Jones, T. A. (1985). *Methods Enzymol.* **115**, 157–171.

Konnert, J. H. & Hendrickson, W. A. (1980). *Computing in Crystallography*, edited by R. Diamond, S. Ramaseshan & K. Venkatesan, pp. 13.01–13.25. Bangalore: Indian Academy of Science.

Krey, G. D., Vanin, E. F. & Swenson, R. P. (1988). *J. Biol. Chem.* **263**, 14436–15443.

Laskowski, R. J., MacArthur, M. W., Moss, D. S. & Thornton, J. M. (1993). *J. Appl. Cryst.* **26**, 283–290.

Lattman, E. E. & Love, W. E. (1972). *Acta Cryst.* B**26**, 1854–1857.

LeGall, J., DerVartanian, D. V. & Peck, H. D. Jr (1979). *Curr. Topics Bioenerg.* **9**, 238–265.

Lennon, B. W., Williams. C. H. Jr & Ludwig, M. L. (1999). *Protein Sci.* **88**, 2366–2379.

Ludwig, M. L., Pattridge, K. A., Metzger, A. L., Dixon, M. M., Eren, M., Feng, Y. & Swenson, R. P. (1997). *Biochemistry*, **36**, 1259–1280.

Massey, V. & Hemmerich, P. (1980). *Biochem. Soc. Trans.* **8**, 246–257.

Mierlo, C. P. M. van, Lijnzaad, P., Vervoort, J., Muller, F., Berendsen, H. J. C. & de Vlieg, J. (1990). *Eur. J. Biochem.* **194**, 185–198.

O'Farrell, P. A., Walsh, M. A., McCarthy, A. A., Higgins, T. M., Voordouw, G. & Mayhew, S.G. (1998). *Biochemistry*, **37**, 8405–8416.

Pflugrath, J. W., Saper, M. A. & Quiocho, F. A. (1985). *Methods and Applications in Crystallographic Computing*, edited by S. Hall & T. Ashiaka, pp. 404–407. Oxford University Press.

Romero, A., Caldeira, J., Legall, J., Moura, I., Moura, J. J. & Romao, M. J. (1996). *Eur. J. Biochem.* **239**(1), 190–196.

Sack, J. S. & Quiocho, F. A. (1997). *Methods Enzymol.* **277**, 159–173.

Sheldrick, G. M. & Schneider, T. R.(1997). *Methods Enzymol.* **277**, 319–343.

Sheriff, S. (1987). *J. Appl. Cryst.* **20**, 55–57.

Sim, G. A. (1960). *Acta Cryst.* **13**, 511–512.

Smith, W. W., Burnett, R. M., Darling, G. D. & Ludwig, M. L. (1977). *J. Mol. Biol.* **117**, 195–225.

Smith, W. W., Pattridge, K. A., Ludwig, M. L., Petsko, G. A., Tsernoglou, D., Tanaka, M. & Yasunobu, K. T. (1983). *J. Mol. Biol.* **165**, 737–755.

Stockman, B. J., Richardson, T. E. & Swenson, R. P. (1994). *Biochemistry*, **33**, 15298–15308.

Swenson, R. P. & Krey, G. D. (1994). *Biochemistry*, **33**, 8505–8514.

Swenson, R. P., Krey, G. D. & Eren, M. (1991). *Flavins and Flavoproteins 1990*, edited by B. Curti, R. Ronchi & G. Zanetti, pp. 415–422. Berlin: Walter de Gruyter.

Watenpaugh, K. D. (1985). *Proceedings of the Molecular Dynamics Workshop, 1984, Chapel Hill*, edited by J. Hermans, pp. 77–80. Western Springs, IL, USA: Polycrystal Books.

Watenpaugh, K. D., Sieker, L. C. & Jensen, L. H. (1973). *Proc. Natl Acad. Sci. USA*, **70**, 3857–3860.

Watt, W., Tulinsky, A., Swenson, R. P. & Watenpaugh, K. D. (1991). *J. Mol. Biol.* **218**, 195–208.